Structure, stability and spectroscopic properties of isomers Of C48B6N6 heterofullerene with isolated and sequential BN substitutional patterns

ARTICLE *in* INORGANICA CHIMICA ACTA · FEBRUARY 2007

Impact Factor: 2.05 · DOI: 10.1016/j.ica.2006.07.101

3 AUTHORS, INCLUDING:

Fabrizia Negri
University of Bologna
160 PUBLICATIONS **3,949** CITATIONS

SEE PROFILE

Available online at www.sciencedirect.com
ScienceDirect
Inorganica Chimica Acta 360 (2007) 1052–1062
Inorganica Chimica Acta
www.elsevier.com/locate/ica

Structure, stability and spectroscopic properties of isomers of $C_{48}B_6N_6$ heterofullerene with isolated and sequential BN substitutional patterns

Emanuela Emanuele, Fabrizia Negri *, Giorgio Orlandi *

Dipartimento di Chimica "G. Ciamician", Università di Bologna, 40126 Bologna, Italy
INSTM UdR Bologna, Bologna, Italy

Received 27 June 2006; accepted 28 July 2006
Available online 12 August 2006

Dedicated to Professor Vincenzo Balzani.

Abstract

Doping of fullerenes has received considerable attention, both experimentally and theoretically, as a tool to fine tuning their physical and chemical properties. In this contribution, we report the results of quantum–chemical calculations on several isomers of the boron and nitrogen doped fullerene derivative $C_{48}B_6N_6$. Optimized structures, relative stability and spectroscopic properties were computed at the B3LYP/6-31G* level of theory. The more stable structures were characterized by computing vibrational frequencies along with Raman and IR intensities and by modeling their absorption spectra with semiempirical and TD-DFT calculations of excitation energies and intensities. Owing to the symmetry lowering with respect to C_{60}, the first allowed transitions of the more stable $C_{48}B_6N_6$ cages appear at lower energies. Despite this, the HOMO–LUMO energy gap, a measure of the semiconducting property, is only slightly reduced, compared to C_{60}. The calculated atomic charge distributions indicate considerable localization of charge on the heteroatoms. As a result, these isomers are expected to have more interesting condensed phase properties than C_{60} owing to their enhanced intermolecular interactions. Among the isomers considered, the reduced structural deformation and favorable electrostatic interactions lead to a preference for the S_6 structure in which two B_3N_3 aggregates are located on opposite hexagons on the cage.

Keywords: Fullerenes; Doped fullerenes; Excited electronic states; IR and Raman spectra; Density functional theory; Semiconductors

1. Introduction

Since the production of the fullerene carbon cages [1,2] several attempts have been made to obtain heteroatom doped analogs. In general, the substitutional doping of aromatic hydrocarbons with heteroatoms can modify substantially the physical and chemical properties of the original hydrocarbons. In a similar way, doping fullerenes with heteroatoms that have different ionization potentials, electron affinities and a different number of electrons with respect to carbon atoms, is expected to modify and tune their electronic, optical, electric and magnetic properties. Furthermore, the substitution of carbon atoms with heteroatoms will modify the electron density distribution on the cage and the intermolecular interactions thereby influencing condensed phase properties of the doped fullerene. The enhanced adsorption of H_2 molecules in light atom doped fullerenes has been recently discussed [3].

The first heterofullerene that was prepared was $C_{59}N$ [4], which being a radical, is highly reactive and forms dimers $(C_{59}N)_2$. Recently, by reactive sputtering of graphite in N_2 a new fullerene material corresponding to the chemical structure $C_{48}N_{12}$ was obtained [5]. This azafullerene contains 12 more electrons than C_{60}. Thus, assuming for $C_{48}N_{12}$ the same orbital sequence of C_{60}, the LUMO t_{1u}

* Corresponding authors. Tel.: +39 0512099471; fax: +39 0512099456 (F. Negri).
E-mail addresses: fabrizia.negri@unibo.it (F. Negri), giorgio.orlandi@unibo.it (G. Orlandi).

0020-1693/$ - see front matter © 2006 Elsevier B.V. All rights reserved.
doi:10.1016/j.ica.2006.07.101

and the LUMO + 1 t_{1g} orbitals of C_{60} are completely filled. Several isomers of $C_{48}N_{12}$ are possible, depending on the positions of the 12 nitrogen atoms on the fullerene surface sites, and each of these structures will have different properties [6]. The structure, vibrational, NMR spectra and electronic spectra of a number of $C_{48}N_{12}$ isomers were discussed in several computational studies [7–13].

Heterofullerenes based on B atoms substitution can also be envisaged as demonstrated by the successful synthesis of $C_{60-n}B_n$ with $1 < n < 6$ [14]. By analogy with azafullerenes, doping with 12 boron atoms has been recently investigated computationally. The B substitution decreases the number of π electrons, which are only 48 in $C_{48}B_{12}$. Assuming the same orbital sequence as in C_{60}, the π electrons fill only four of the five orbitals of h_g parentage leaving the 5th empty. The physical and chemical properties of the few isomers of $C_{48}B_{12}$ have been considered [15–17] with the motivation that $C_{48}B_{12}$ and $C_{48}N_{12}$ are promising components of molecular rectifiers [17,18].

Since $(BN)_n$ clusters are currently attracting much interest for their great stability [19–24], the doping of carbon cages with B and N atoms appears a promising way to improve the physical and chemical properties of fullerenes. The substitutional doping follows, in this case, the $BN \leftrightarrow C_2$ rule and the best candidates have therefore the general formula $C_{60-2n}B_nN_n$. In contrast with $C_{48}B_{12}$ and $C_{48}N_{12}$, BN doped fullerenes contain the same number of π electrons as C_{60} and thus, they are expected to have, in some respect, similar electronic properties. Boron–nitrogen substitution patterns in C/BN hybrid fullerenes have been investigated with semiempirical and density functional theory (DFT) calculations [25–27]. Structure, stability and spectroscopic properties of four isomers of $C_{48}B_6N_6$ have been recently examined in detail with DFT calculations [28]. Recently, theoretical predictions of the nucleus independent chemical shift (NICS) of $C_{48}B_{12}$, $C_{48}N_{12}$ and $C_{48}B_6N_6$ have been presented [29–31].

In this paper we present DFT calculations on several isomers of $C_{48}B_6N_6$ to determine their structures, stabilities and ionization energies. Previous theoretical studies have concerned $C_{48}B_6N_6$ isomers with isolated B and N dopants distributed on the cage [28], isolated BN couples [28] or B_nN_n aggregates localized on the cage [25,32]. Here we consider structures with isolated BN couples similar to that investigated in Ref. [28] but we also investigate isomers with an increasing dimension of B_nN_n aggregates such as B_2N_2, B_3N_3 and B_6N_6. Besides structural characteristics and energy order, we also derive IR and Raman activities to establish whether the different isomers can be distinguished on the basis of their vibrational spectra. Vertical electronic excitation energies and transition dipole moments are computed for the three lowest energy isomers to ascertain whether they are significantly dependent on the specific isomer. The computed structural, electronic and spectral properties will contribute to clarify whether $C_{48}B_6N_6$ doped fullerenes may be valuable components for molecular electronic devices.

2. Methods

Ground state energies and structures of $C_{48}B_6N_6$, along with normal modes and vibrational frequencies, were calculated with DFT, using the B3LYP exchange – correlation hybrid functional [33,34] and the standard 6-31G* basis set. Geometry optimization was refined with the Opt = Tight and Int = UltraFine options. Electronic energies and transition dipole moments were obtained at the B3LYP/6-31G* equilibrium structures by using the CNDO/S semiempirical Hamiltonian [35,36] which was widely employed in the study of several unsaturated molecules and, particularly, to successfully interpret both the singlet and triplet state spectroscopy of C_{60} and C_{70} [37–39]. The Self-Consistent-Field (SCF) calculation of Molecular Orbitals (MOs) was followed by a Configuration Interaction (CI) calculation in which only Singly Excited Configurations (SECs) were taken into account. The two-center electron repulsion integrals were evaluated according to the Mataga-Nishimoto (MN) approximation. The CI treatment included about 1600 SECs.

To check the validity of this description we performed CI calculations of different sizes and did not find any appreciable differences in the energy ordering of the lowest electronic states, for CI including more than 500 configurations. Electronic excitation energies were evaluated also by employing the time-dependent (TD) version of DFT [40], using the same B3LYP functional [33] and basis set. All the DFT calculations were carried out with the GAUSSIAN 03 suite of programs [41]. Atomic charges were computed with two methods: from the standard Mulliken population analysis and by fitting the electrostatic potential according to the ESP procedure [42].

3. Results

3.1. Structure and electronic properties of $C_{48}B_6N_6$

While in $C_{48}N_{12}$ [6] and $C_{48}B_{12}$ [6] fullerenes the heteroatoms tend to distribute themselves among the carbon atoms, the opposite electron affinities of Boron and Nitrogen favor the formation of $C_{48}(BN)_6$ structures in which the two B and N heteroatoms come in couples (BN) or in larger aggregates (such as B_2N_2 and B_3N_3). Owing to the remarkable stability of B_nN_n clusters, among the $C_{48}B_6N_6$ isomers considered in this work we have included not only structures of the $C_{48}(BN)_6$ type, in which the BN couples are isolated, but also structures in which the B and N atoms form B_2N_2, B_3N_3 and B_6N_6 aggregates. We carried out B3LYP/6-31G* calculations to obtain the optimized structures, absolute and relative energies of the 10 isomers shown in Figs. 1 and 2, labeled **A**, **B**, ..., **L** according to their predicted energy order, which is summarized in Table 1.

The two lowest energy isomers, **A** and **B**, have two B_3N_3 aggregates and are characterized by two borazine-like substructures $B_3N_3H_6$ on the opposite hexagons of the cage.

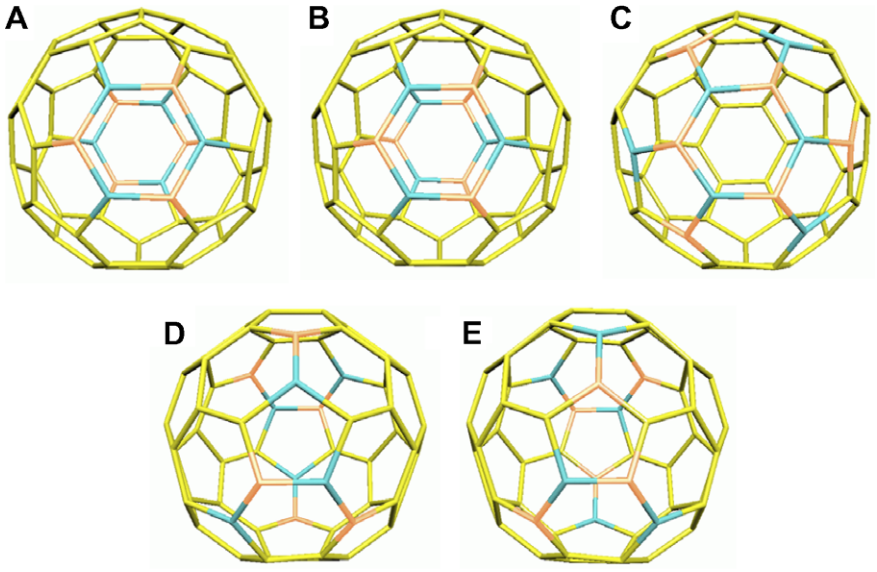

Fig. 1. B3LYP/6-31G* optimized structures of isomers **A**, **B**, **C**, **D**, **E** of $C_{48}B_6N_6$. Nitrogen atoms are orange, boron atoms blue and carbon atoms yellow. (For interpretation of the references in color in this figure legend, the reader is referred to the web version of this article.)

Isomer **A** belongs to the S_6 symmetry group while isomer **B** belongs to D_3 symmetry group (see Fig. 1) and the dipole moment is zero in both isomers by symmetry. The energy of the **B** isomer is computed to be 2.9 kcal/mol higher than that of isomer **A**, as a result of repulsive interactions between pairs of identical dopants (B or N) on the two opposite borazine-like substructures (see Fig. 1). Isomer **C** has one B_6N_6 aggregate located on and around one hexagon (see Fig. 1). It belongs to the C_3 symmetry group and accordingly its non-zero dipole moment was calculated to be 1.57 D. The energy of this isomer is 10.8 kcal/mol above isomer **A**. The next two isomers, **D** and **E**, are characterized by the presence of two B_2N_2 aggregates and two isolated BN couples. Each B_2N_2 sequence is located on a hexagon, with the central BN occupying a pentagon–hexagon bond. On the same pentagon is located also one end of an isolated BN couple connecting two pentagons, such that the heteroatom on the three-substituted pentagon is separated from the other two BN atoms by one carbon atom (see Fig. 1). The remaining B_2N_2 sequence and the isolated BN couple are distributed with the same motif repeated on the opposite pentagon (see Fig. 1). The arrangement is such that there are two B and one N atom on the same pentagon in isomer **D** and two N and one B atom in isomer **E**. Therefore, both isomers belong to the C_i symmetry group. The relative energies of the optimized **D** and **E** structures are computed to be 75.4 kcal/mol and 85 kcal/mol above isomer **A**, respectively. We note, in passing, that lower symmetry isomers with the same motif around the two opposite pentagons can be obtained by simply exchanging a BNBN with a NBNB sequence, inverting the BN couple, or by doing both operations, on one of the two pentagons. This results in a family of isomers with energies close to those of the two symmetric members (isomer **D** and **E**).

The following five isomers, **F**, **G**, **H**, **I**, and **L**, depicted in Fig. 2, have six non-interacting BN couples distributed on the fullerene surface such that each BN couple occupies a hexagon–hexagon bond joining two pentagons. There are three pairs of BN dipoles on the opposite sides of the cage, each pair oriented perpendicularly to the remaining two (see Fig. 2). Thus, the five isomers in Fig. 2 are characterized by the same motif, but they differ in the reciprocal orientation of the six BN couples. Isomers **F** and **G** belong to the S_6 symmetry group and hence have a zero dipole moment. Furthermore, each pair of BN couples experiences an attractive dipolar interaction because the two BN dipoles are antiparallel (see Fig. 2). In contrast, isomers **H**, **I** and **L** have either no symmetry element (isomers **H** and **I**) or one C_3 axis (isomer **L**) and their non-zero dipole moments are predicted to be 0.55, 0.84 and 1.09 D, respectively. These three isomers are characterized by an increasing number of repulsive parallel BN dipoles on the opposite sides of the cage: one pair of parallel BN opposite dipoles in isomer **H**, two pairs in isomer **I** and three pairs in isomer **L**. The energies of these five isomers range from 113.5 to 118.1 kcal/mol above isomer **A**. According to their similar structure and dipolar interactions, the energies of the two isomers **F** and **G** differ by only 0.3 kcal/mol, while those of isomers **H**, **I** and **L** increase in the order, by about the same amount of ca. 1.5 kcal/mol. Such an energy increase can be rationalized by considering that the main difference between the two sequential isomers in the family is an additional repulsive interaction between two BN dipoles. In a previous study on $C_{48}(BN)_6$, four isomers were considered [28]. Only isomer 1 of Ref. [28] was characterized by B and N atoms distributed as BN couples, each couple joining two different pentagons in the cage as in the family **F**–**L** described above. In isomer 2 of Ref. [28], nitrogen atoms were included in the three pentagons,

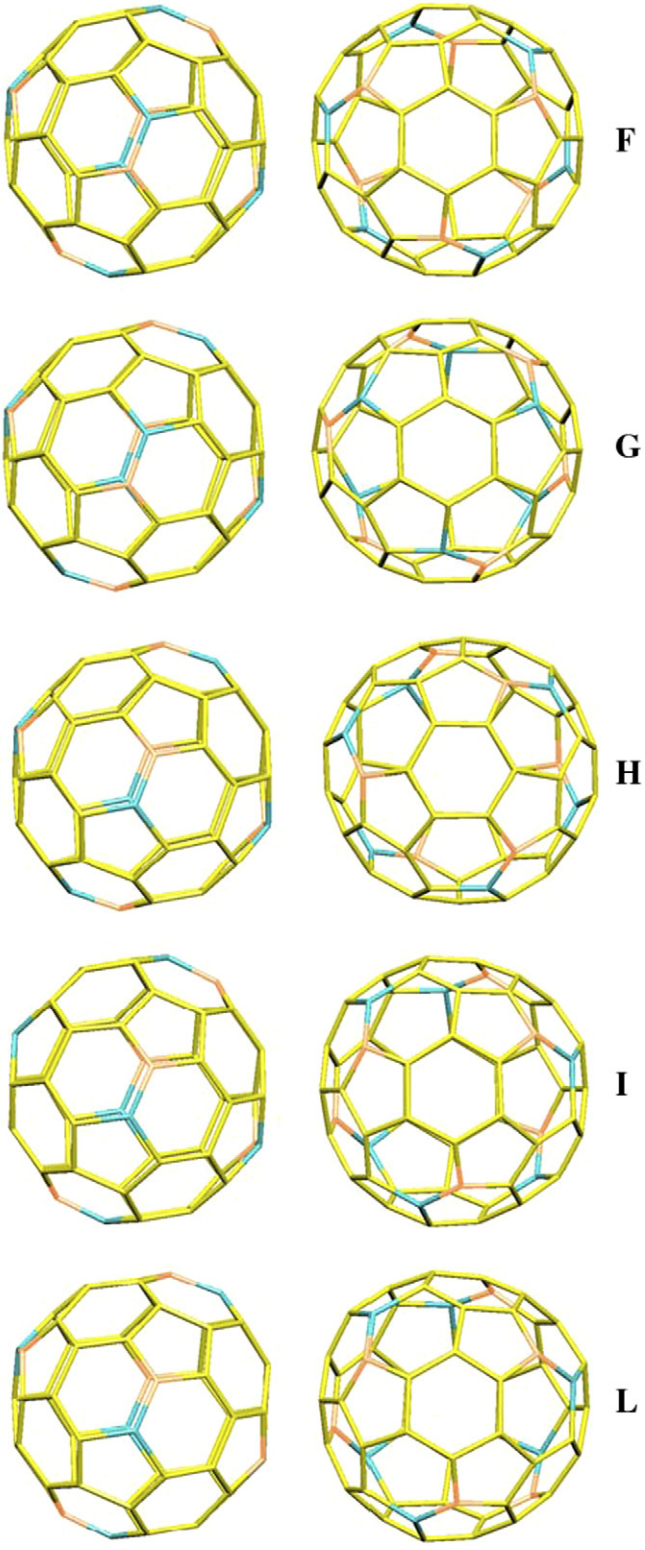

Fig. 2. B3LYP/6-31G* optimized structures of isomers **F**, **G**, **H**, **I**, **L** of $C_{48}B_6N_6$. Nitrogen atoms are orange, boron atoms blue and carbon atoms yellow. (For interpretation of the references in color in this figure legend, the reader is referred to the web version of this article.)

one heteroatom per pentagon, enclosing each of the two triphenylene units on the opposite sides of the cage, while the boron atoms were distributed along the equator. In isomer 3, the B and N atoms were exchanged with respect to isomer 2 whilst in isomer 4, boron and nitrogen atoms were distributed in the same positions as the N atoms in the Stafstrom $C_{48}N_{12}$ structure [6]. Isomers 2, 3, 4 were found to be at a much higher energy than isomer 1 [28]. Notice that the latter isomer coincides with our isomer **H**, which is 115.2 kcal/mol higher than our most stable isomer (isomer **A**).

Table 1
B3LYP/6-31G* energies of the $C_{48}B_6N_6$ isomers at their optimized structures

Isomer	Sym	Energy (a.u.)	Relative energy (kcal/mol)
A	S_6	−2306.99375	0.0
B	D_3	−2306.98909	2.9
C	C_3	−2306.97648	10.8
D	C_i	−2306.87350	75.5
E	C_i	−2306.85821	85.1
F	S_6	−2306.81283	113.5
G	S_6	−2306.81235	113.8
H[a]	C_1	−2306.81023	115.2
I	C_1	−2306.80790	116.6
L	C_3	−2306.80554	118.1

[a] This isomer corresponds to the lowest energy structure investigated in Ref. [28].

Owing to the large energy range covered by the isomers considered in this work, in the following we restrict the description of structural details and charge distributions only to the more stable isomers of $C_{48}B_6N_6$. The labeling of the relevant bonds (in red) and atom centers (in black) is defined in Fig. 3 where we make use of the same C_{60} Schlegel diagram for the three isomers. The central hexagon in the Schlegel diagram corresponds to the top central hexagon of isomers **A**, **B** and **C** in Fig. 1. The corresponding B3LYP/6-31G* computed equilibrium bond lengths (Å) are collected in Table 2. As expected, in all three isomers, the CC bond lengths are, on average, close to the two values, roughly 1.40 Å and 1.45 Å, which are typical of C_{60} hexagon–hexagon and hexagon–pentagon bonds, respectively. In the **A** and **B** isomers the CC hexagon–pentagon bond lengths assume values ranging from 1.44 to 1.47 Å, while the hexagon–hexagon bond lengths range from 1.39 to 1.40 Å. The BN bonds, located on the borazine-like substructures, assume two values, 1.48 and 1.44 Å, depending on their pentagon–hexagon or hexagon–hexagon type. The CN and BC bonds are all of the pentagon–hexagon type: the latter bond lengths are 1.53 Å and 1.43 Å respectively. In isomer **C**, where heteroatoms are clustered on and around one hexagonal ring, BN bonds are located on the ring or are oriented radially with respect to the ring. The BN bonds on the BN ring are 1.43 Å or 1.46 Å long, depending on the nature (hexagon or pentagon) of the adjacent ring. The radial BN bonds are all of hexagon–pentagon type, but their lengths assume two values, 1.47 Å or 1.51 Å, depending on the nature, N or B, of the atom in the heteroatomic ring. The BC bond lengths of isomer **C** are 1.50 Å or 1.55 Å for hexagon–hexagon and pentagon–hexagon bonds, respectively. The CN

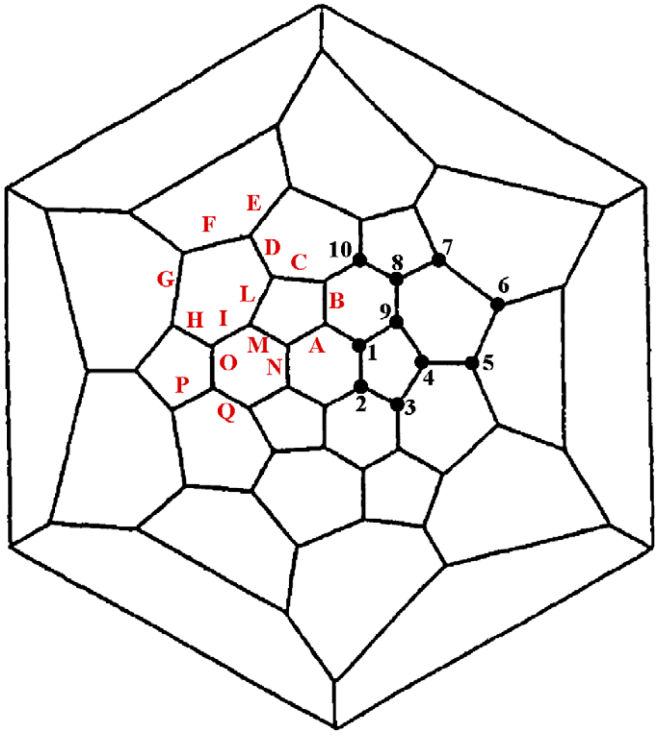

Fig. 3. Schlegel diagram of C_{60}. The diagram is employed to identify selected atomic centers (labeled in black with numbers) and bond lengths (labeled in red with letters) for the more stable isomers **A**, **B** and **C** of $C_{48}B_6N_6$. The central hexagon in the Schlegel diagram corresponds to the top central hexagon of the three isomers in Fig. 1. (For interpretation of the references in color in this figure legend, the reader is referred to the web version of this article.)

bond lengths are 1.38 Å or 1.43 Å depending on their type. The bond lengths of isomers **A**, **B** and **C** cannot be compared with those reported in Ref. [28] since these isomers were not considered. The energy and structure and other molecular properties computed for our isomer **H** do, however, coincide with those of isomer 1 of Ref. [28]. Owing to the distribution of N and B atoms, the two **A** and **B** isomers of $C_{48}B_6N_6$ have a slightly ellipsoid shape, because the principal axis (C_3) is not equivalent to the other two axes perpendicular to it.

Table 2
B3LYP/6-31G* equilibrium bond lengths (Å) of the three more stable (isomers **A**, **B**, **C**) $C_{48}B_6N_6$ isomers

Bond[a]	Isomer **A**	Isomer **B**	Isomer **C**
A	BN 1.478	BN 1.477	BN 1.462
B	CN 1.431	CN 1.435	BN 1.470
C	CC 1.461	CC 1.456	BC 1.546
D	CC 1.402	CC 1.403	CC 1.381
E	CC 1.447	CC 1.448	CC 1.477
F	CC 1.454	CC 1.447	CC 1.447
G	CC 1.401	CC 1.404	CC 1.388
H	CC 1.453	CC 1.444	CC 1.453
I	CC 1.386	CC 1.385	CN 1.383
L	CC 1.439	CC 1.442	CN 1.425
M	BC 1.524	BC 1.527	BN 1.507
N	BN 1.438	BN 1.437	BN 1.429
O	CC 1.473	CC 1.472	CC 1.418
P	CC 1.453	CC 1.456	CC 1.460
Q	CC 1.394	CC 1.392	BC 1.499

[a] Bond labels according to Fig. 3.

In contrast to C_{60}, the charge of $C_{48}B_6N_6$ isomers is not distributed uniformly on the fullerene cage because of the different electronegativity of N, B and C atoms. In Table 3 we collected, according to the labels shown in Fig. 3, the more relevant Mulliken and ESP [42] atomic charges evaluated at B3LYP/6-31G* level of theory for isomers **A**, **B** and **C**. The ESP charges are more significant in the discussion of intermolecular interactions, and are the result of a fitting procedure aimed to reproduce the electrostatic potential in regions close to the molecular surface. Thus, they are a useful tool to evaluate intermolecular interactions. In isomer **A**, the Mulliken (ESP) atomic charges for carbon atoms linked to N and B atoms are 0.17 (0.34) and −0.07 (−0.48), respectively. The Mulliken (ESP) charges on N and B atoms are −0.47 (−0.70) and 0.39 (0.79), respectively. The Mulliken charges for carbon atoms that are not directly bound to B or N atoms are quite small (less than 0.01), but ESP charges for these

Table 3
Mulliken and ESP atomic charges of the three more stable $C_{48}B_6N_6$ isomers

Isomer **A**				Isomer **B**			Isomer **C**		
Atom		Mulliken[b]	ESP[b]	Atom type	Mulliken[b]	ESP[b]	Atom type	Mulliken[b]	ESP[b]
No.[a]	Type								
1	B	0.39	0.79	B	0.39	0.76	B	0.53	0.83
2	N	−0.47	−0.70	N	−0.47	−0.68	N	−0.45	−0.79
3	C	0.17	0.34	C	0.17	0.27	B	0.18	0.55
4	C	−0.01	0.05	C	−0.01	0.05	C	0.15	−0.12
5	C	0.00	−0.01	C	0.00	−0.02	C	−0.03	0.06
6	C	−0.01	0.16	C	0.01	−0.02	C	0.03	0.13
7	C	0.01	−0.19	C	0.01	−0.02	C	−0.01	−0.14
8	C	−0.01	0.36	C	−0.01	0.24	C	0.19	0.49
9	C	−0.07	−0.48	C	−0.07	−0.39	N	−0.53	−0.37
10	C	−0.01	−0.33	C	−0.01	−0.27	C	−0.03	−0.60

[a] Atom numbers according to Fig. 3.
[b] Charges computed from B3LYP/6-31G* wavefunctions.

atoms may be sizeable (for example, 0.16 and −0.19). Similar charges are computed for isomer **B**. The dipole moment of both the isomers is zero. In isomer **C**, where B and N atoms are clustered on and around one hexagon ring, the Mulliken (ESP) charges on N atoms are −0.45 (−0.79) and −0.53 (−0.37) for N atoms in the ring and around it, respectively. Correspondingly, the charges on B atoms are 0.53 (0.83) and 0.18 (0.55) for atoms in the ring and around it, respectively. This charge distribution generates a sizeable dipole moment of 1.57 D along the C_3 axis, with the negative end on the BN ring. In isomer **D**, which can be defined as $C_{48}(B_2N_2)_2(BN)_2$, the charges on the isolated BN couples are 0.23 and −0.50, respectively, while the charges on the atoms the BNBN aggregate are 0.26, −0.44, 0.40 and −0.52, respectively. The charges on C atoms range from 0.22 to 0.19 for atoms bound to N and from −0.66 to −0.07 for atoms bound to B atoms. The charges on carbons bound to two B atoms are −0.12. In isomer **F**, which is the most stable isomer of the $C_{48}(BN)_6$ family described above, the Mulliken charges on N atoms are −0.49 and the charges on B atoms are 0.27. The charges of carbon atoms close to N are 0.22 and 0.20, while those of C atoms close to boron are −0.07 and −0.06. Other C atoms have charges of about −0.02 e.

Owing to the charged atoms in the $C_{48}B_6N_6$ cage, this heterofullerene should show stronger interactions with the solvent molecules and, thus, a better solubility than C_{60}. These charges should also produce stronger interactions between closely packed $C_{48}B_6N_6$ molecules and give origin to a more stable solid phase than C_{60}. The stronger intermolecular interactions, accompanied by a tighter binding, should influence the electronic properties of the solid phase improving intermolecular energy and charge transfer.

Ionization potentials and electron affinities are important molecular properties that affect the electronic spectra and the occurrence of charge transfer processes. The first ionization potential and the first electron affinity correlate with the energies of the HOMO and of the LUMO, respectively. The B3LYP/6-31G* computed HOMO and LUMO energies of the isomers considered in this work are collected in Table 4 and compared with the values computed for the previously investigated heterofullerenes $C_{48}B_{12}$, $C_{48}N_{12}$ and for C_{60}. The HOMO energies of the different isomers **A**–**L** lie in the range −5.62 eV (isomer **E**) −5.88 eV (isomer **F**) while the LUMO energies lie in the range −3.20 eV (isomer **B**) −2.86 eV (isomer **F**). As a result, the HOMO, LUMO and the energy gaps (*E*(LUMO)–*E*(HOMO)) of isomers **A**–**E** are rather similar, whilst those of isomer **F** are distinctly different not only when compared with the five lowest energy isomers quoted above, but also when compared to the other four members (isomers **G**–**L**) belonging to the same family of $C_{48}(BN)_6$ isomers with isolated BN couples. In particular, the energy gap of the **F** isomer stands out as the largest in the considered collection of isomers. In practice, the most relevant values are those that are computed for the **A**, **B** and **C** isomers, which are the more stable structures. These have almost identical energy gaps, but isomer **C** has slightly higher HOMO and LUMO energies. While comparing the $C_{48}(BN)_6$ isomers with C_{60}, $C_{48}N_{12}$ and $C_{48}B_{12}$ cages we notice that the HOMO and LUMO energies are similar to those of C_{60}, with the gap being slightly smaller (2.56–2.60 versus 2.77 eV). $C_{48}N_{12}$ has the highest HOMO and LUMO energies but an energy gap very similar to that of C_{60}. $C_{48}B_{12}$ has the lowest LUMO energy and thus the smallest energy gap.

Table 4
B3LYP/6-31G* HOMO, LUMO and Δ*E*(LUMO–HOMO) energies of the $C_{48}B_6N_6$ isomers at their optimized structures and comparison with C_{60} and related heterofullerenes

Isomer	*E*(HOMO) (eV)	*E*(LUMO) (eV)	Δ*E*
A	−5.78	−3.18	2.60
B	−5.76	−3.20	2.56
C	−5.65	−3.11	2.54
D	−5.58	−3.19	2.39
E	−5.62	−3.06	2.56
F	−5.88	−2.86	3.02
G	−5.63	−2.99	2.64
H	−5.71	−2.99	2.72
I	−5.76	−3.03	2.73
L	−5.84	−3.02	2.82
C_{60}	−5.99[a]	−3.22[a]	2.77
$C_{48}N_{12}$	−4.90[a]	−2.16[a]	2.74
$C_{48}B_{12}$	−5.69[a]	−4.08[a]	1.61

[a] From Ref. [18].

3.2. Vibrational spectra of the more stable $C_{48}B_6N_6$ isomers

In icosahedral C_{60} there are only 46 distinct frequencies out of the 174 normal modes and of these, only four bands (528, 577, 1183, 1429 cm^{-1}) belonging to the t_{1u} symmetry species are observed in IR spectra and only 10 bands (497, 1469 cm^{-1} of a_g type and 273, 437, 710, 774, 1099, 1250, 1428, 1575 cm^{-1} of h_g type) are recorded in the Raman spectrum. The lower symmetry of $C_{48}B_6N_6$ isomers implies a lower degeneracy and a larger number of distinct vibrational frequencies. Correspondingly, a richer structure is expected for the IR and Raman spectra of these doped fullerenes. For instance, isomer **A**, belonging to the S_6 symmetry point group, has 58 distinct frequencies (of A_u and E_u symmetry) that may be active in IR and 58 (of A_g and E_g symmetry) that may show up in the Raman spectra. Rather than giving the list of frequencies and intensities, we depicted in Figs. 4–10 the resulting IR and Raman spectra of isomers **A**–**G**, obtained from B3LYP/6-31G* computed vibrational frequencies and intensities.

A cursory inspection of the computed spectra indicates that (i) The IR and Raman spectra of all the $C_{48}B_6N_6$ are quite rich in bands. The simplest are, not surprisingly, those computed for isomers **A**, **F** and **G**, namely the highest symmetry isomers considered in this work. These spectra are, however, sufficiently distinct to allow one to distinguish and identify the different isomers. (ii) For all the

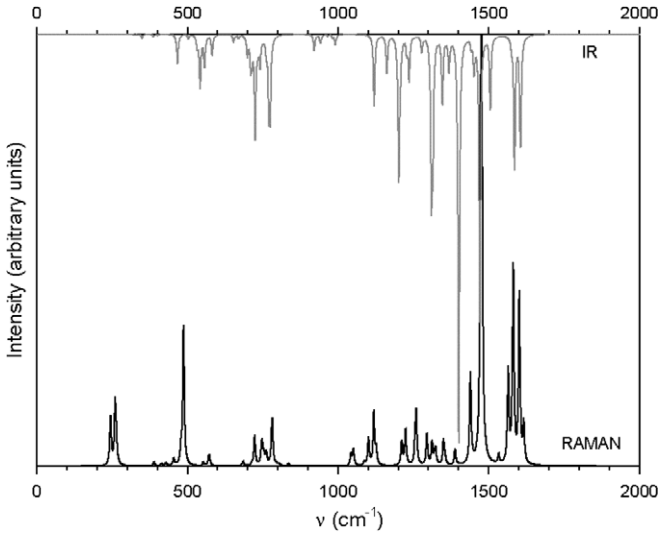

Fig. 4. IR and Raman spectra of the $C_{48}B_6N_6$ isomer **A** simulated with the computed B3LYP/6-31G* frequencies and intensities.

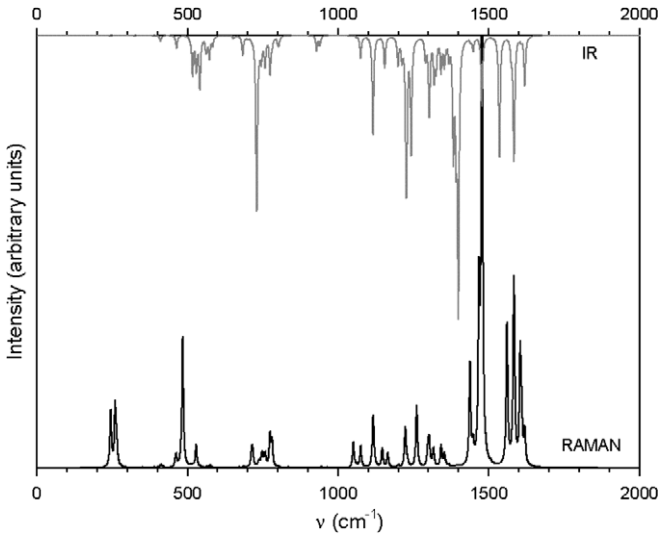

Fig. 5. IR and Raman spectra of the $C_{48}B_6N_6$ isomer **B** simulated with the computed B3LYP/6-31G* frequencies and intensities.

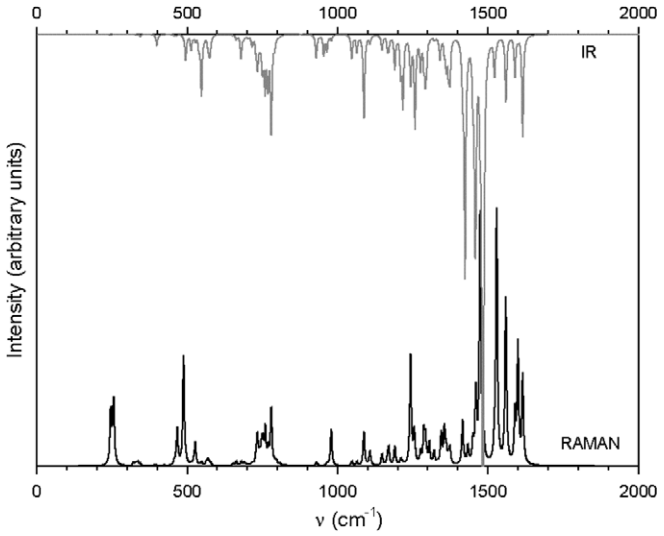

Fig. 6. IR and Raman spectra of the $C_{48}B_6N_6$ isomer **C** simulated with the computed B3LYP/6-31G* frequencies and intensities.

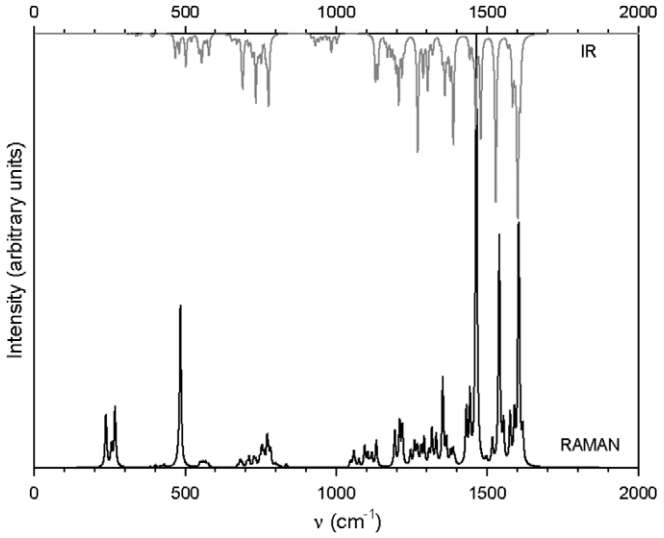

Fig. 7. IR and Raman spectra of the $C_{48}B_6N_6$ isomer **D** simulated with the computed B3LYP/6-31G* frequencies and intensities.

$C_{48}B_6N_6$ isomers we note that, compared to C_{60}, the IR intensity shifts toward higher frequencies. This effect is presumably due to the large dipole moments of the BN bonds, which preferentially enhance the intensity of the local, high frequency modes. The richness of the IR spectra of $C_{48}B_6N_6$ isomers indicates a substantial transfer of intensity to modes that are silent in C_{60}, that is modes not derived from the t_{1u} modes of C_{60}. This effect is a direct consequence of the symmetry lowering that follows the substitutional doping with N and B atoms. (iii) Considering the Raman spectra, it can be noted that the modes related with the a_g modes of C_{60}, which dominate the Raman activity of buckminsterfullerene, show up with strong intensity also in the spectra of $C_{48}B_6N_6$ isomers. However, also the intensities of modes of h_g parentage are quite strong and, furthermore, modes of g_g and of other g parentage, Raman allowed in the doped fullerene, show considerable activities. In particular, bands close to 1600 cm^{-1} appear among the most intense in all the $C_{48}B_6N_6$ isomers.

3.3. Electronic spectra

A large molecule with 60 second row atoms, like C_{60} (or $C_{48}B_6N_6$), possesses a large number of electronic excited states in the visible and near UV region. For instance, a calculation based only on the SECs generated from 120 occupied and 120 unoccupied valence MOs, leads to 14400 states. For this reason, most calculations of excitation energies and oscillator strengths for the lower excited states of

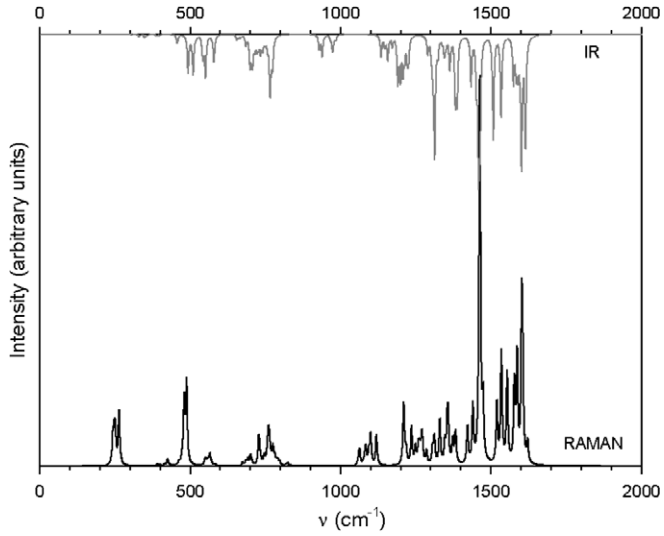

Fig. 8. IR and Raman spectra of the $C_{48}B_6N_6$ isomer **E** simulated with the computed B3LYP/6-31G* frequencies and intensities.

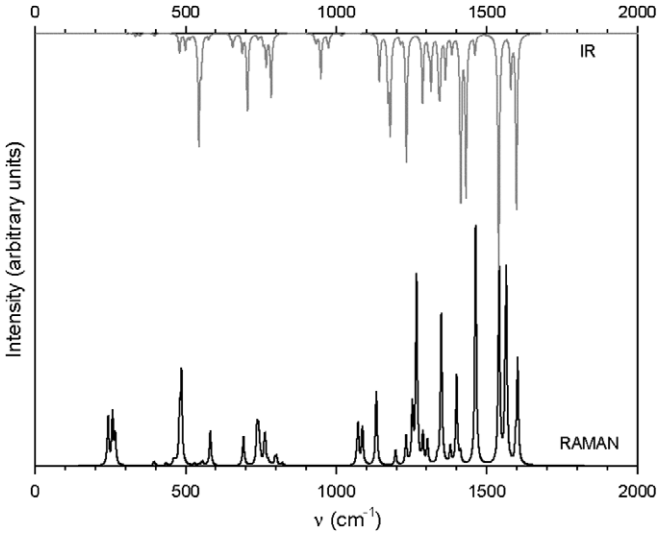

Fig. 10. IR and Raman spectra of the $C_{48}B_6N_6$ isomer **G** simulated with the computed B3LYP/6-31G* frequencies and intensities.

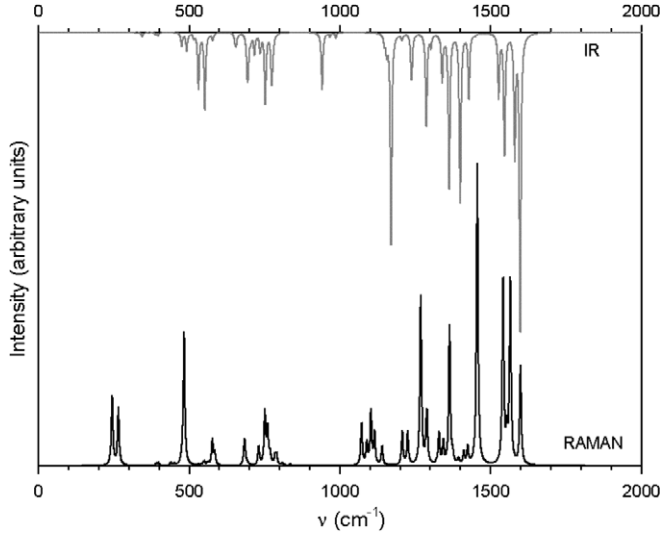

Fig. 9. IR and Raman spectra of the $C_{48}B_6N_6$ isomer **F** simulated with the computed B3LYP/6-31G* frequencies and intensities.

C_{60} were based on semiempirical Hamiltonians, such as CNDO/S and INDO/S, and on CI treatments involving up to about 1000 SECs. Calculations of this size provided a realistic description of the lowest electronic states of fullerenes [37–39]. An alternative approach is based on the use of time-dependent (TD) DFT, which was already applied to fullerenes [43].

We analyzed the visible near UV spectrum of $C_{48}B_6N_6$ by using both the CNDO/S-CI and the TD-DFT methods and we considered only the three lowest energy isomers, namely, **A**, **B** and **C**. The next isomer, **D**, which is 75 kcal/mol above isomer **A**, seems unlikely to be found in the synthesis. We performed the CNDO/S calculations followed by CI calculations that included the 42X42 MOs space (1764 SECs) for isomer **A**, the 42X48 MOs space (2016 SECs) for isomer **B** and the 46X42 MOs space (1932 SECs) for isomer **C**. Furthermore, we predicted the visible and near UV spectrum also with TD-DFT (B3LYP/6-31G*) calculations limited to the lowest 30 singlet excited states, that is, up to about 3.5 eV.

The absorption spectra, modeled using singlet state energies and oscillator strengths computed, for the lowest energy isomers, with CNDO/S followed by CI calculations, are shown in Fig. 11. A Lorentian linewidth of 0.1 eV was superimposed to each computed electronic transition. In Table 5 we collected the TD-DFT excited singlet state energies and oscillator strengths.

Owing to the similar electronic structure, it is convenient to compare the predicted electronic excitation spectra of the $C_{48}B_6N_6$ isomers with the spectrum of C_{60}. In contrast, apparent analogies with $C_{48}N_{12}$ would be misleading because the electronic excitations of the latter involve different orbitals. Considering the lowest predicted states, up to 3.5 eV, both TD-DFT and CNDOS + CI calculations indicate a shift of the lowest excited electronic states of the three $C_{48}B_6N_6$ isomers toward lower energies, with respect to C_{60}. The lowest excited state is predicted to be below 2.0 eV for all the three isomers. The CNDO/S calculations predict an even larger energy lowering, a result that is probably connected with an unbalanced parametrization of the B atom (in the presence of N atoms). The manifold of electronic levels is very dense, when compared to C_{60}, because the states belonging to $T_{1g/u}$, $T_{2g/u}$, $G_{g/u}$, $H_{g/u}$ in icosahedral symmetry are each split into a number of $A_{g/u}$ (A or A_1 and A_1) and $E_{g/u}$ (E) states, in the lower S_6 (D_3 or C_3) symmetry point group. For the same reason, in contrast to C_{60}, many transitions from the ground state to excited states are formally allowed in $C_{48}B_6N_6$ isomers, and occur without requiring a vibronic borrowing mechanism. As indicated in Table 5, the first allowed transition is computed at a

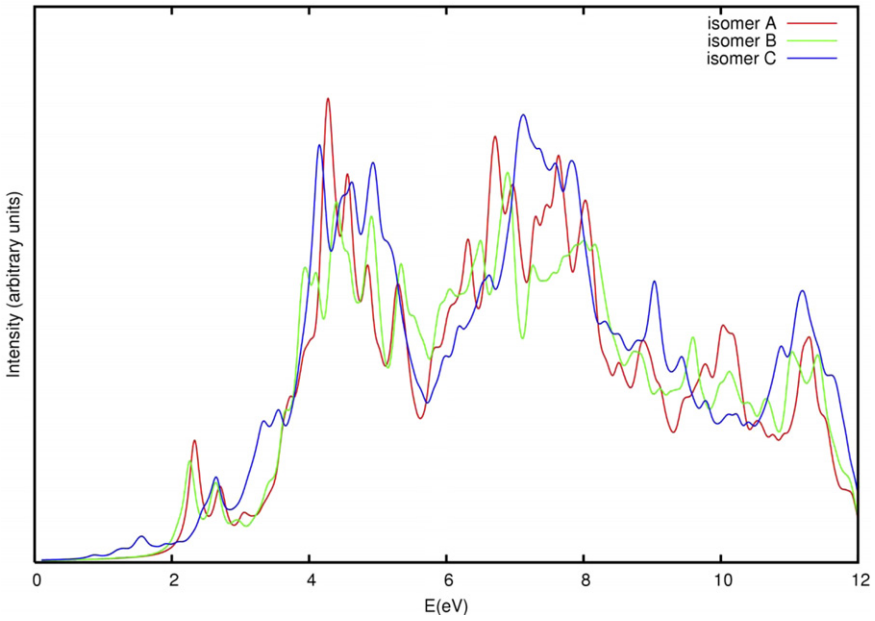

Fig. 11. $S_0 \rightarrow S_n$ absorption spectra of the three more stable $C_{48}B_6N_6$ isomers, **A**, **B** and **C**, simulated with the computed CNDO/S + CI vertical excitation energies and intensities.

Table 5
TD-DFT (B3LYP/6-31G*) energies (eV), oscillator strengths *f* and symmetry of the lowest singlet electronic states of the three more stable isomers of $C_{48}B_6N_6$

Isomer **A**			Isomer **B**			Isomer **C**		
Sym	*E* (eV)	*f*	Sym	*E* (eV)	*f*	Sym	*E* (eV)	*f*
$2A_g$	1.945	0.000	$2A_1$	1.900	0.000	2A	1.863	0.000
$1E_g$	1.992	0.000	1E	1.985	0.000	1E	1.895	0.001
$3A_g$	2.380	0.000	$3A_1$	2.288	0.000	3A	1.951	0.000
$2E_g$	2.419	0.000	2E	2.331	0.007	2E	1.976	0.010
$4A_g$	2.520	0.000	$1A_2$	2.386	0.000	4A	2.018	0.004
$3E_g$	2.562	0.000	3E	2.390	0.000	3E	2.046	0.002
$1E_u$	2.925	0.012	4E	2.509	0.017	5A	2.452	0.000
$4E_g$	2.948	0.000	$2A_2$	2.699	0.000	4E	2.515	0.009
$1A_u$	3.052	0.000	5E	2.743	0.001	6A	2.539	0.001
$2E_u$	3.123	0.002	$4A_1$	2.780	0.007	5E	2.603	0.005
$2A_u$	3.163	0.000	$3A_2$	3.205	0.000	7A	2.905	0.000
$3E_u$	3.195	0.001	6E	3.208	0.000	6E	2.918	0.006
$3A_u$	3.289	0.004	$5A_1$	3.228	0.002	8A	2.941	0.005
$5E_g$	3.300	0.000	7E	3.263	0.000	7E	3.009	0.001
$5A_g$	3.301	0.000	8E	3.364	0.027	9A	3.043	0.009
$4A_u$	3.324	0.004	$6A_1$	3.367	0.009	8E	3.044	0.005
$6A_g$	3.324	0.000	$4A_2$	3.383	0.000	10A	3.078	0.001
$5A_u$	3.352	0.001	9E	3.443	0.008	9E	3.164	0.044
$4E_u$	3.364	0.063	$7A_1$	3.481	0.019	11A	3.383	0.000
$5E_g$	3.420	0.015	10E	3.597	0.008	10E	3.425	0.015

lower energy than in C_{60} for all the three isomers **A**, **B** and **C**. The first strong electronic transition occurs, according to TD-DFT calculations, at 3.36, 3.36 and 3.16 eV for the **A**, **B** and **C** isomers, respectively. These energies are surprisingly similar to those of the first T_{1u} state of C_{60} obtained by TD-DFT [43].

The wider energy range covered by the CNDO/S + CI predictions (see Fig. 11) is convenient to compare the spectra of the three isomers of $C_{48}B_6N_6$ in the higher energy region. The intense bands of **A**, **B** and **C** isomers at ~3.4, 4.0 and 4.3 eV correspond to the transitions to the $1T_{1u}$, $2T_{1u}$ and $3T_{1u}$ states of C_{60}, respectively. Among the three, isomer **C** shows the lowest electronic states and the largest absorption in the visible region. Owing to the availability of many low energy excited states, isomer **C** is expected to be strongly polarizable.

From the computed excited state properties, it can be concluded that in solid or thin film phases, these doped fullerenes are expected to be better semiconductors than C_{60} owing to their smaller S_0–S_1 energy gap.

4. Conclusions

We have considered several isomers of the boron nitride doped fullerene $C_{48}B_6N_6$ and we have identified new structures with remarkably lower energies than those considered in a recent study [28]. In particular we have found that the lowest energy isomer corresponds to two borazine-like substructures located on the opposite sides of the cage, such that each B (N) atom on one borazine substructure interacts preferentially with one N (B) atom on the opposite substructure.

All the computed isomers are characterized by remarkable charges localized on the boron and nitrogen atoms. The significant charges computed on several atoms imply a stronger interaction with solvent molecules and therefore a better solubility compared with C_{60}. Furthermore, in the solid phase, stronger interactions are expected between molecules that may result in better transport properties.

Owing to the presence of lower energy singlet excited states (compared to C_{60}) the $C_{48}B_6N_6$ isomers are expected to have more promising semiconductor properties.

The different $C_{48}B_6N_6$ isomers have different stabilities and the specific electronic and spectroscopic properties that should allow us to discriminate unambiguously among the isomers.

Acknowledgements

This work was supported by funds from MURST PRIN 2004 (Project: ''Spettroscopia rotazionale in assorbimento e a trasformate di Fourier: Produzione e studio di nuovi cluster e specie molecolari in espansioni supersoniche''), MURST PRIN 2005 (Project: ''Trasferimenti di energia e di carica a livello molecolare''), MURST ex 60% (Project: ''Modelli per lo studio delle proprietà di sistemi molecolari complessi'') and FIRB 2001 (Project: ''Carbon based micro and nanostructures'', RBNE019NKS).

References

[1] H.W. Kroto, J.R. Heath, S.C. O' Brien, R.F. Curl, R.E. Smalley, Nature 318 (1985) 162.
[2] W. Kratschmer, L.D. Lamb, K. Fostiropoulos, D.R. Huffman, Nature 347 (1990) 354.
[3] Y.H. Kim, Y.F. Zhao, A. Williamson, M.J. Heben, S.B. Zhang, Phys. Rev. Lett. 96 (2006) 016102.
[4] J.C. Hummelen, B. Knight, J. Pavlovich, R. Gonzalez, F. Wudl, Science 269 (1995) 1554.
[5] L. Hultman, S. Stafstrom, Z. Czigany, J. Neidhardt, N. Hellgren, I.F. Brunell, K. Suenaga, C. Colliex, Phys. Rev. Lett. 8722 (2001) 225503.
[6] S. Stafstrom, L. Hultman, N. Hellgren, Chem. Phys. Lett. 340 (2001) 227.
[7] M.R. Manaa, D.W. Sprehn, H.A. Ichord, J. Am. Chem. Soc. 124 (2002) 13990.
[8] M.R. Manaa, D.W. Sprehn, H.A. Ichord, Chem. Phys. Lett. 374 (2003) 405.
[9] R.H. Xie, G.W. Bryant, L. Jensen, J.J. Zhao, V.H. Smith, J. Chem. Phys. 118 (2003) 8621.
[10] R.H. Xie, G.W. Bryant, V.H. Smith, Phys. Rev. B: Condens. Mat. 67 (2003) 155404.
[11] R.H. Xie, G.W. Bryant, V.H. Smith, Chem. Phys. Lett. 368 (2003) 486.
[12] E. Emanuele, F. Negri, G. Orlandi, Chem. Phys. 306 (2004) 315.
[13] B. Schimmelpfennig, H. Agren, S. Csillag, Synth. Met. 132 (2003) 265.
[14] T. Guo, C.M. Jin, R.E. Smalley, J. Phys. Chem. 95 (1991) 4948.
[15] R.H. Xie, L. Jensen, G.W. Bryant, J.J. Zhao, V.H. Smith, Chem. Phys. Lett. 375 (2003) 445.
[16] M.R. Manaa, H.A. Ichord, D.W. Sprehn, Chem. Phys. Lett. 378 (2003) 449.
[17] R.H. Xie, G.W. Bryant, J.J. Zhao, V.H. Smith, A. Di Carlo, A. Pecchia, Phys. Rev. Lett. 90 (2003) 206602.
[18] M.R. Manaa, Chem. Phys. Lett. 382 (2003) 194.
[19] S.H. Xu, M.Y. Zhang, Y.Y. Zhao, B.G. Chen, J. Zhang, C.C. Sun, Chem. Phys. Lett. 423 (2006) 212.
[20] S.H. Xu, M.Y. Zhang, Y.Y. Zhao, B.G. Chen, J. Zhang, C.C. Sun, Chem. Phys. Lett. 418 (2006) 297.
[21] J. Kunstmann, A. Quandt, J. Chem. Phys. 121 (2004) 10680.
[22] R.R. Zope, T. Baruah, M.R. Pederson, B.I. Dunlap, Chem. Phys. Lett. 393 (2004) 300.
[23] M. Machado, P. Piquini, R. Mota, Chem. Phys. Lett. 392 (2004) 428.
[24] T. Oku, A. Nishiwaki, I. Narita, Phys. B Condens. Mat. 351 (2004) 184.
[25] J. Pattanayak, T. Kar, S. Scheiner, J. Phys. Chem. A 105 (2001) 8376.
[26] J. Pattanayak, T. Kar, S. Scheiner, J. Phys. Chem. A 106 (2002) 2970.
[27] T. Kar, J. Pattanayak, S. Scheiner, J. Phys. Chem. A 107 (2003) 8630.
[28] M.R. Manaa, R.H. Xie, V.H. Smith, Chem. Phys. Lett. 387 (2004) 101.
[29] Z.F. Chen, R.B. King, Chem. Rev. 105 (2005) 3613.
[30] Z.F. Chen, H.J. Jiao, D. Moran, A. Hirsch, W. Thiel, P.V. Schleyer, J. Phys. Org. Chem. 16 (2003) 726.
[31] Z.F. Chen, H.J. Jiao, A. Hirsch, A. Thiel, J. Org. Chem. 66 (2001) 3380.
[32] Z.F. Chen, K.Q. Ma, H.X. Zhao, Y.M. Pan, X.Z. Zhao, A.C. Tang, J.K. Feng, J. Mol. Struct. Theochem. 466 (1999) 127.
[33] A.D. Becke, J. Chem. Phys. 98 (1993) 5648.
[34] C. Lee, W. Yang, R.G. Parr, Phys. Rev. B: Condens. Mat. 37 (1988) 785.
[35] J. Del Bene, H.H. Jaffe', J. Chem. Phys. 48 (1968) 4050.
[36] C.A. Masmanidis, H.H. Jaffe', R.L. Ellis, J. Phys. Chem. 79 (1975) 19.
[37] F. Negri, G. Orlandi, F. Zerbetto, J. Chem. Phys. 97 (1992) 6496.
[38] A. Sassara, G. Zerza, M. Chergui, F. Negri, G. Orlandi, J. Chem. Phys. 107 (1997) 8731.
[39] G. Orlandi, F. Negri, Photochem. Photobiol. Sci. 1 (2002) 289.
[40] M.E. Casida, C. Jamorski, K.C. Casida, D.R. Salahub, J. Chem. Phys. 108 (1998) 4439.
[41] M.J. Frisch, G.W. Trucks, H.B. Schlegel, G.E. Scuseria, M.A. Robb, J.R. Cheeseman, J.A. Montgomery Jr., T. Vreven, K.N. Kudin, J.C. Burant, J.M. Millam, S.S. Iyengar, J. Tomasi, V. Barone, B. Mennucci, M. Cossi, G. Scalmani, N. Rega, G.A. Petersson, H. Nakatsuji, M. Hada, M. Ehara, K. Toyota, R. Fukuda, J. Hasegawa, M. Ishida, T. Nakajima, Y. Honda, O. Kitao, H. Nakai, M. Klene, X. Li, J.E. Knox, H.P. Hratchian, J.B. Cross, C. Adamo, J. Jaramillo, R. Gomperts, R.E. Stratmann, O. Yazyev, A.J. Austin, R. Cammi, C. Pomelli, J.W. Ochterski, P.Y. Ayala, K. Morokuma, G.A. Voth, P. Salvador, J.J. Dannenberg, V.G. Zakrzewski, S. Dapprich, A.D. Daniels, M.C. Strain, O. Farkas, D.K. Malick, A.D. Rabuck, K. Raghavachari, J.B. Foresman, J.V. Ortiz, Q. Cui, A.G. Baboul, S. Clifford, J. Cioslowski, B.B. Stefanov, G. Liu, A. Liashenko, P. Piskorz, I. Komaromi, R.L. Martin, D.J. Fox, T.

Keith, M.A. Al-Laham, C.Y. Peng, A. Nanayakkara, M. Challacombe, P.M.W. Gill, B. Johnson, W. Chen, M.W. Wong, C. Gonzalez, J.A. Pople, GAUSSIAN 03, Revision C.02, Gaussian, Inc., Wallingford CT, 2004.

[42] B.H. Besler, K.M. Merz, P.A. Kollman, J. Comput. Chem. 11 (1990) 431.

[43] R. Bauernschmitt, R. Ahlrichs, F.H. Hennrich, M.M. Kappes, J. Am. Chem. Soc. 120 (1998) 5052.